



OPEN ACCESS

EDITED BY
Alan R Butcher,
Geological Survey of Finland, Finland

REVIEWED BY
Duncan Pirrie,
University of South Wales,
United Kingdom
Carlos Duarte Simões,
University of Algarve, Portugal

*CORRESPONDENCE
I Ward,
ingrid.ward@uwa.edu.au

SPECIALTY SECTION
This article was submitted to Quaternary
Science, Geomorphology and
Paleoenvironment,
a section of the journal
Frontiers in Earth Science

RECEIVED 16 December 2021
ACCEPTED 07 September 2022
PUBLISHED 28 September 2022

CITATION
Ward I, McDonald J, Monks C and
Fairweather J (2022), Use of micro-
analysis to augment the macro-
archaeological investigation of an
elevated Holocene shell midden,
Dampier Archipelago, NW Australia.
Front. Earth Sci. 10:837338.
doi: 10.3389/feart.2022.837338

COPYRIGHT
© 2022 Ward, McDonald, Monks and
Fairweather. This is an open-access
article distributed under the terms of the
[Creative Commons Attribution License
\(CC BY\)](https://creativecommons.org/licenses/by/4.0/). The use, distribution or
reproduction in other forums is
permitted, provided the original
author(s) and the copyright owner(s) are
credited and that the original
publication in this journal is cited, in
accordance with accepted academic
practice. No use, distribution or
reproduction is permitted which does
not comply with these terms.

Use of micro-analysis to augment the macro-archaeological investigation of an elevated Holocene shell midden, Dampier Archipelago, NW Australia

I Ward^{1*}, J McDonald^{1,2}, C Monks¹ and J Fairweather³

¹School of Social Sciences, University of Western Australia, Crawley, WA, Australia, ²CRAR+M, School of Social Sciences, University of Western Australia, Crawley, WA, Australia, ³School of Earth and Planetary Sciences, Curtin University, Bentley, WA, Australia

Few studies in Australia have employed automated mineral techniques to augment archaeological site investigations, and there are no known published micromorphological studies of Australian shell midden sites. This pilot study presents results of a micro-analytical investigation of a *Tegillarca granosa* (formerly known as *Anadara granosa*) midden in the Old Geos site, located in an elevated location on the Burrup Peninsula in NW Australia. Analytical investigations were undertaken on a 15 cm profile in the upper section dated to 1,500 cal yr BP of a 50 cm excavation profile that has a maximum age estimate of around 7,000 cal yr BP. Although invertebrate activity has reduced the temporal and spatial resolution, mineralogical analyses differentiate a higher relative concentration of alkali feldspars in the top of the sampled profile consistent with freshly weathered granophyre bedrock, as well as presence of rare rutilitic quartz. The profile otherwise shows sediment source and transport has remained constant. In addition to the shell, cultural material includes fish, mammal and possibly avian bone, some of which have been burnt. Plant material is limited but does include micro-fragments of charcoal and phytoliths from grass and wood. Fungal tissue is further evidence of present or past degrading organic matter. Both this, and a previous micro-analytical study on the more distant site of Barrow Island, highlight how micro-analytical investigation can provide more detail on depositional and post-depositional history of midden and other archaeological records in this region.

KEYWORDS

shell midden analysis, automated mineral analysis, micromorphology, Dampier Archipelago, Australia, TIMA analyses

1 Introduction

Located in the coastal Pilbara, the Dampier Archipelago (including the Burrup Peninsula), now generally known as Murujuga, hosts one of the most significant long-term records of Aboriginal symbolic and economic adaptation to fluctuating sea levels in Australia, with over a million rock art engravings, numerous stone structures, middens, quarries and other occupational remains (McDonald and Veth 2009; McDonald et al., 2018; Beckett 2021). The archipelago's formation is relatively recent, following post-glacial inundation of the arid coastal plain around 9,000 years ago (Ward et al., 2013). In contrast, the igneous bedrock geology formed at the end of the Archean era over 2700 million years ago, and comprises granophyre and gabbro over a granite base (Donaldson 2011). Granophyre and gabbro form the steep scree-strewn hills on which much of the rock art is found (McDonald and Veth 2009; Donaldson 2011).

In 2017, an excavation was undertaken on the Burrup Peninsula at an open site known as Old Geos (Figure 1), so named for the extensive older assemblage of geometric rock art found here (Berry 2018). Micromorphological and associated automated mineral analysis (using TESCAN instrumentation) was primarily undertaken to complement the macro-scale archaeology and to help understand site formation history. As highlighted by Ward et al. (2018), very few studies in Australia

have employed automated mineral techniques to archaeological site investigations, and there are no known published micromorphological studies of shell midden sites. This paper presents the results of these analyses to aid interpretation of site formation and stratigraphy; and, building on similar work undertaken in the broader region (Ward et al., 2017, 2018), discusses the potential of microanalytical and automated mineral analysis to augment understanding of past and present processes in ancient archaeological sites of arid Australia.

1.1 Old Geos excavation site

The Old Geos site is an extensive open site complex that includes engravings, shallow shell midden and artefact scatters, grinding patches, and stone structures (mostly low stacked circular constructions). The site is located on a plateau approximately 50 m above sea level in the centre of the southern Burrup Peninsula (Murujuga), approximately 2 km from both east and west coasts (Figure 1). The extensive *Tegillarca* sp. (blood cockle; previously known as *Anadara granosa*) midden covers 1,300 m² on an elevated, gently sloping (<5°) area, immediately north of an ephemeral creek and rock hole. Middens, shell and earth mounds dominated by *Tegillarca* occur throughout the coastal Pilbara, and generally date from the mid to late Holocene (Clune and Harrison 2009; Morse 2009). This Old Geos midden is only unusual because of its elevated and interior location, near an ephemeral freshwater source. Two 1 × 1 m excavation squares (named OG 044686 and OG 028690) were excavated at this site, the first (Square OG 028690) in the centre of the extensive open *Tegillarca* sp. midden, and the second (OG 044686) inside one of the eight circular stone structures located on the northeastern edge of the midden site (see McDonald et al., 2022).

The micromorphological study was focused on excavation square OG 028690. This excavation was dug in eight arbitrary units (or spits, XU) of 8–10 cm depth, with cultural shell occurring mainly at the top of the sequence and artefacts occurring right down to a boulder base (Figure 2). Based on field observations on the distribution of shell, inferred stratigraphic units and chronological dates (see below), two analytical units (AU) were designated:

- AU1 (XU1 – 3), 0–25 cm. This unit comprising densely-packed *Tegillarca granosa* shell (95% total shell volume), with minor quantities (<1% total shell volume) of other edible taxa, including *Saccostrea* sp., *Acanthopleura* sp. (chiton), *Telescopium* sp., crustacea and also non-dietary *Melo amphora*. Both flaked artefacts (90% total artefact volume) and bone (75% total bone volume) are more abundant in this upper unit.
- AU2 (XU4 – 8), 25–45 cm. This unit comprises only 3% of the total shell in this excavation square. It has similar taxa

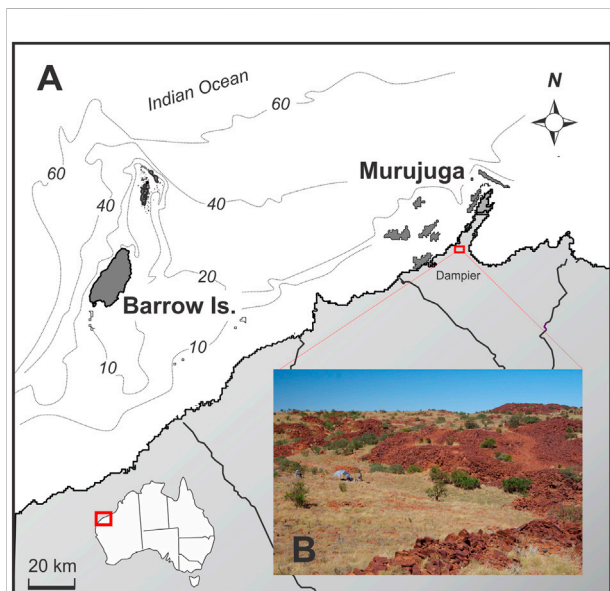
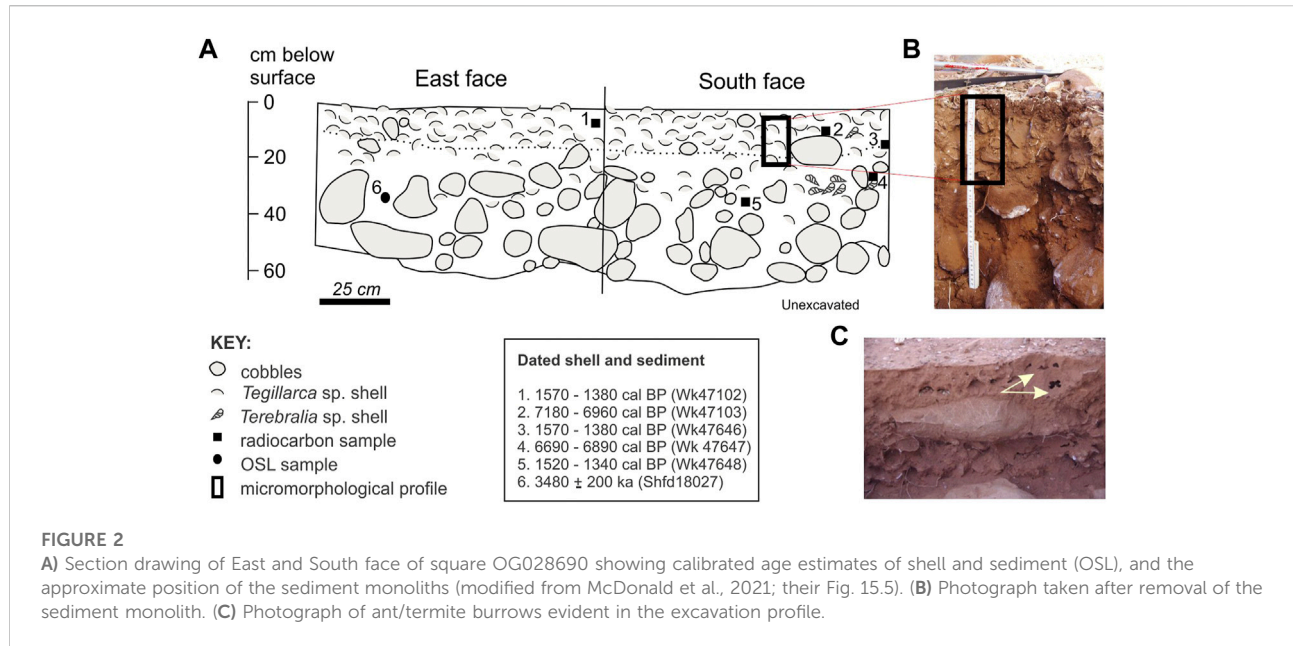


FIGURE 1

A). Location of Old Geos midden site in the central part of Burrup Peninsula, in the coastal Pilbara region of NW Australia. (B). Photograph of the saddle on which the Old Geos midden site is located. The ephemeral creek line is marked by the line of green trees behind the excavation area located underneath the tent.



as in the overlying unit, but highly fragmented *Tegillarca granosa* shell accounts for <10% of this and *Terebralia* sp. accounts for over 50% of the shell by weight in this unit (McDonald et al., 2022: Table 15.8).

While the distribution of shell and artefacts are described as two stratigraphic units, distinct lithostratigraphic units are distinguished only by an increase in volume and size of granophyre blocks (cobble and boulder sized), and more intense red colouration and compaction of sediments with depth. The more red-brown colour (7.5 YR 3/3) at the surface compared to the deeper sediments (5 YR 3/4) reflects the higher organic and lower moisture content of the upper sediments. Acidity increases with depth from pH 7.5 near the surface to 6.5 at depth. Within the moderate-well sorted ferruginous fine sandy sediments, there is clear evidence of termite activity right through to the base of the profile, including open and infilled passages, black faecal matter (frass), and possible cadaverous remains.

A summary diagram of the excavation profile is provided in Figure 2 and includes calibrated age estimates from radiocarbon dating of selected *Tegillarca* sp. ($n = 3$) and *Terebralia* sp. ($n = 2$) shell and also optically-stimulated luminescence (OSL) dating ($n = 1$) of sediments at 35 cm depth. Bayesian modelling indicates a maximum age of the deposit of around 7 ky BP, with *Terebralia* sp. shell at 12 cm (Wk47103) and 25 cm (Wk47647) depth dated between 7,180–6,600 cal yr BP, within sediments dated by OSL to 3.5 ± 0.2 ka (Shfd18027) using small aliquot dating (McDonald et al., 2022). These are overlain by the *Tegillarca* sp. shell with a modelled age between 1,310–1,160, including a displaced shell from XU5 (AU2) (Wk47648). Similar age estimates were

obtained for *Tegillarca* sp. shell from excavation square OG 044686, with OSL age estimates ranging from 5.2 ± 0.2 ka at 32 cm depth (Shfd18030) to 1.2 ± 0.1 ka at 14 cm depth (Shfd18028). These two analytical units, which represent disparate cultural occupation events in first the mid-Holocene, followed by that in the Late Holocene reveal some chronostratigraphic mixing. Given the gentle sloped surface, it is likely that sediments and associated cultural material will have infilled the cobble and boulder surface, possibly over multiple episodes and with ongoing reworking by ants and termites, with the surface gradually levelling out over time. A non-linear age-depth chronology is therefore highly probable. Full details of this excavation, and the archaeological and chronological dating sampling and results from this are provided by McDonald et al. (2022).

2 Methodology

2.1 Field sampling and micromorphological preparation

A single block of sediment was taken from the South wall of the excavation profile in the upper shell-rich unit (CU1), at approximately 0–20 cm vertical depth on the southern wall (Figure 2). Due to the densely-packed nature of the cobbles and boulders, it was not possible to take a micromorphological sample from the lower unit, although the interface between the two is captured at the base of the block. Bulk sediment samples were collected down the profile to aid sediment characterization, in particular from particle size distribution (of the <2 mm

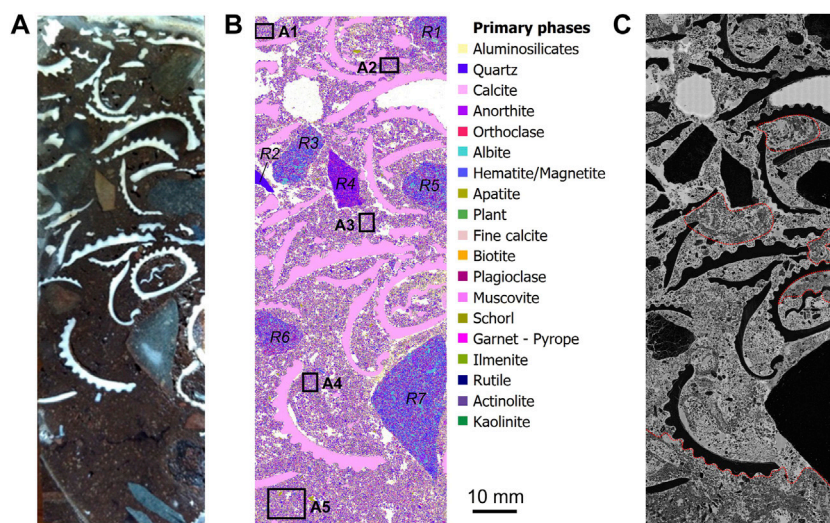


FIGURE 3

A) Scan of the resin-impregnated section of shell midden, used for TIMA analysis. **(B)** TIMA mineral map showing distribution of main mineral phases, with minerals in order of abundance listed in the legend. Selected rocks (R1 – R7) and areas of sediment matrix (A1 – A4) that were also analytically sub-sampled by TMA are also marked. **(C)** The mineral map of carbon shows the inhomogenous nature of the sedimentary matrix, with areas preserving evidence of faunal (ant/termite) activity outlined in red. Note areas of very high contrast reflect pore spaces with resin.

fraction) using the Malvern Mastersizer 2000 housed at the University of Western Australia (UWA).

The plaster-encased sediment block was transported back to UWA for processing and analysis. Sediment monoliths were air-dried before resin impregnation, using a polyester resin/styrene mixture, and then allowed to cure over several weeks. The hardened monoliths were cut into blocks using a diamond rock saw. A slice ($13 \times 5 \times \sim 8$ cm) was cut from the block, and polished on one side to be used for quantitative mineral analysis (Figure 3), and a further slice was cut to make thin sections (2.5×5 cm) 25–30 microns-thick to profile the stratigraphy.

2.2 Quantitative mineralogical analyses and micromorphology

The large (13×8 cm) polished section of the resin-impregnated block was analysed using a TESCAN TIMA SEM-EDS system at the John de Laeter Centre at Curtin University. The TESCAN Integrated Mineral Analyser (TIMA) operating system comprises a scanning electron microscope fitted with four silicon drift energy dispersive X-ray spectrometers (SEM-EDS), to quantitatively determine the mineralogical composition of sediments (Pirrie et al., 2004; Haberlah et al., 2011; Ward et al., 2018).

TIMA analyses were run using the high-resolution liberation analysis mode with the sample surface automatically mapped using a fixed step interval set at $10 \mu\text{m}$. Elemental spectra and

BSE signal were captured using the TESCAN TIMA software with a spot size set at 46 nm , a working distance of 15 mm and a field size set at $1,500 \mu\text{m}$. The spectroscopic data was matched to mineral definition files within the TIMA classification scheme (using Version 2.4.2 TIMA software) to create digital pixel maps of mineral assemblages (Ward et al., 2018), with the addition of a ‘resin’ and ‘plant’ classification from an EDS signal collected on identified examples of these phases. Modal mineral abundances were determined for the whole block. In addition, analytical sub-sampling of five (5) areas (Figure 3) focused on the groundmass between the shell matrix to explore any mineral trends through the profile. Further details of the TIMA operating system can be found in Hrstka et al. (2018) and Ward et al. (2018).

Studies indicate it might be possible to differentiate shell types by chemistry (Wan Mohammad et al., 2017), hence an attempt was made to differentiate shell species by TIMA analysis. Elemental spectra and BSE signal were captured (spot size of $44\text{--}73 \text{ nm}$) on 10 different shell types, including both marine and terrestrial shell, from an existing micromorphological reference collection (refer Ward et al., 2019). No significant difference was observed in the elemental abundance of the different shell types, although decalcification and contamination with aluminosilicate minerals was evident in the archaeological specimen of *Terebralia* sp. compared to the modern sample. Hence, shell types were differentiated, where possible, from micromorphological observation rather than from TIMA analysis. All thin sections were observed using in a Nikon Eclipse LV100ND petrographic microscope under plane polarized light (PPL) and crossed-polarized light (XPL) using

TABLE 1 Modal percentages of each of the primary phases within selected areas of the midden profile and also for and for large rock fragments within the profile.

Primary Phases	Shell slab	Area 1	Area 2	Area 3	Area 4	Area 5	Area average	Area SD	Rock average	Rock SD
Aluminosilicates	31.48	35.75	39.01	46.09	42.83	43.19	41.37	4.03	12.7	5.03
Quartz	24.90	26.56	26.94	31.29	31.25	28.50	28.91	2.27	43.4	18.79
Calcite	7.12	14.15	11.69	11.33	10.28	9.07	11.30	1.89	0.0	0.00
Orthoclase (KAlSi ₃ O ₈)	22.95	13.21	11.81	0.34	0.11	4.35	5.96	6.23	10.4	4.23
Albite (NaAlSi ₃ O ₈)	5.60	5.42	5.51	5.97	6.83	6.46	6.04	0.61	18.7	10.98
Hematite/Magnetite	5.67	2.38	2.53	2.77	3.77	2.98	2.88	0.54	1.5	0.93
Anorthite (CaAl ₂ Si ₂ O ₇)	1.15	0.60	1.06	0.72	3.79	3.66	1.96	1.62	7.2	6.49
Apatite	0.33	0.82	0.33	0.37	0.20	0.90	0.52	0.32	0.0	0.00
Plant	0.26	0.46	0.49	0.55	0.25	0.25	0.40	0.14	0.0	0.00
Fine calcite	0.12	0.16	0.08	0.11	0.21	0.10	0.13	0.05	0.0	0.00
Plagioclase	0.07	0.05	0.10	0.04	0.15	0.07	0.08	0.04	0.2	0.14
Biotite	0.08	0.07	0.05	0.07	0.07	0.10	0.07	0.02	0.3	0.22
Ilmenite	0.04	0.08	0.10	0.04	0.04	0.05	0.06	0.03	0.0	0.01
Muscovite	0.03	0.07	0.06	0.04	0.07	0.06	0.06	0.01	0.0	0.01
Garnet—pyrope	0.03	0.08	0.08	0.07	0.03	0.04	0.06	0.03	0.0	0.01
Rutile	0.03	0.05	0.03	0.05	0.06	0.06	0.05	0.01	0.0	0.01
Schorl	0.03	0.02	0.03	0.04	0.03	0.08	0.04	0.03	0.0	0.02
Actinolite	0.02	0.04	0.03	0.04	0.01	0.01	0.03	0.01	0.0	0.01
Kaolinite	0.01	0.01	0.01	0.03	0.01	0.01	0.01	0.01	0.0	0.05
Titanite	0.01	0.00	0.01	0.02	0.00	0.01	0.01	0.01	0.0	0.02
Zircon	0.01	0.00	0.01	0.02	0.00	0.02	0.01	0.01	0.0	0.00
The rest	0.02	0.01	0.00	0.00	0.01	0.02	0.01	0.00	0.01	0.00
Total	100.00	100.00	100.00	100.00	100.00	100.00				

different magnifications (2×, 5×, 10×, 25×), and broadly described from [Stoops \(2003\)](#).

3 Results

3.1 Tescan integrated mineral analyser

3.1.1 Shell slab

It was not possible to achieve a complete TIMA analysis of the entire shell midden slab due to electrical charging in the lowermost 2 cm. This unfortunately reflects incomplete coating due to the size of the slab being at the limit of the chamber of the carbon coater. Subsequent post-analytical analysis was limited to the remainder of the profile as shown in [Figure 3](#). The modal mineral abundances for Old Geos show a significantly higher relative abundance of K-feldspar (orthoclase) and lower relative abundance of quartz, calcite and aluminosilicates (clay mineral mixtures with varying abundances of Al, Si, K, Na, Ca, Mg, Fe, Zn peaks in the EDS spectra that do not fit the end-member definitions of illite, montmorillonite, etc.) in the whole shell

profile, compared to selected areas (A1—A5) ([Figure 4](#); [Table 1](#)). The modal mineral abundance of the whole shell profile may be partly influenced by the rock fragments, the majority of which have a high alkali feldspar content (~10% orthoclase, ~19% albite) and correspond to a granophyre or a chemical equivalent such as granite, granodiorite or rhyodacite (R1, R3, R4, R6, R7). Rock 5 (R5) is most likely an arkosic sandstone and Rock 2 a quartz sandstone.

The modal mineral abundances of the sedimentary matrix (i.e., the sediments between the embedded calcitic shell) are predominantly composed of aluminosilicate clays (41%), quartz (29%), calcite (likely as small shell fragments, 11%) and fine calcite (as calcite cement, <0.2%) and feldspars (orthoclase, albite, anorthite; 14%) ([Table 1](#)). Minor phases include inosilicates (e.g., actinolite/ferro-actinolite, titanate, hornblende) and mica (biotite, muscovite), and clay (kaolinite) reflecting the weathering and metamorphic products of the local sub-volcanic source rock. Possible cultural material includes burnt (charcoal) and unburnt plant (~0.4%), and also apatite as bone (0.5%). Although modal apatite is a common minor mineral in felsic igneous

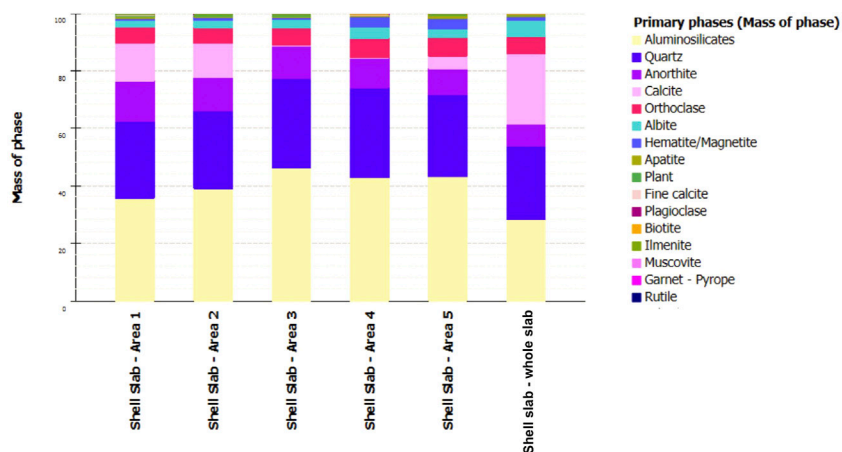


FIGURE 4
Summary of modal mineral abundances through the Old Geos slab, including whole slab and from sub-sampled areas of the groundmass through the profile.

rocks (Piccoli and Candela, 2002), the occurrence of apatite as bone in the sediment matrix rather than as an accessory mineral in the lithic clasts is consistent with microscope observations (see below).

Modal abundances from the selected areas show a minerogenic change between the top few centimetres of the profile (A1 and A2) compared to the rest of the profile (A3–A5), with a relative increase in aluminosilicates (>42%), quartz (>31%), iron-oxides (~3%), Ca-feldspar (>3%) and a significant decrease in K-feldspar (from >11% to <4%) (Figure 5). There is also a lower relative abundance of plant (0.25%) in the base of the profile that may reflect the slightly

more acidic conditions. The modal abundance of bone apatite is highest at the base of the profile (0.9%) but is otherwise variably distributed.

Reworking of the sedimentary matrix is indicated from the higher relative concentration of aluminosilicates (shown as pale yellow in Figure 3C), and also the lower relative concentration of carbon (C) (shown as areas of lower contrast in Figure 3C). Localised areas where the sedimentary fabric has been ‘rotated’ (Figure 3C) further indicate bioturbation, most likely by ants or termites whose galleries and black corpses remains are evident even at the macroscale. These reworked areas are concentrated on the right side and base of the slab (Figure 3).

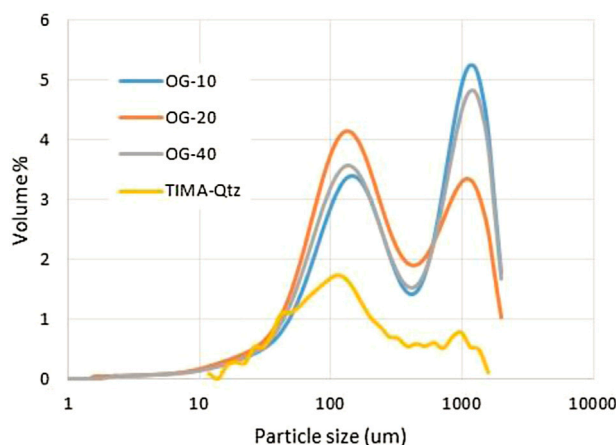


FIGURE 5
Summary of laser particle size analysis (Mastersizer) at 10 cm, 20 and 40 cm in the Old Geos excavation, and for quartz as determined by TIMA. Both analyses show two main modes at 120–150 μm and 1,000–1,250 μm.

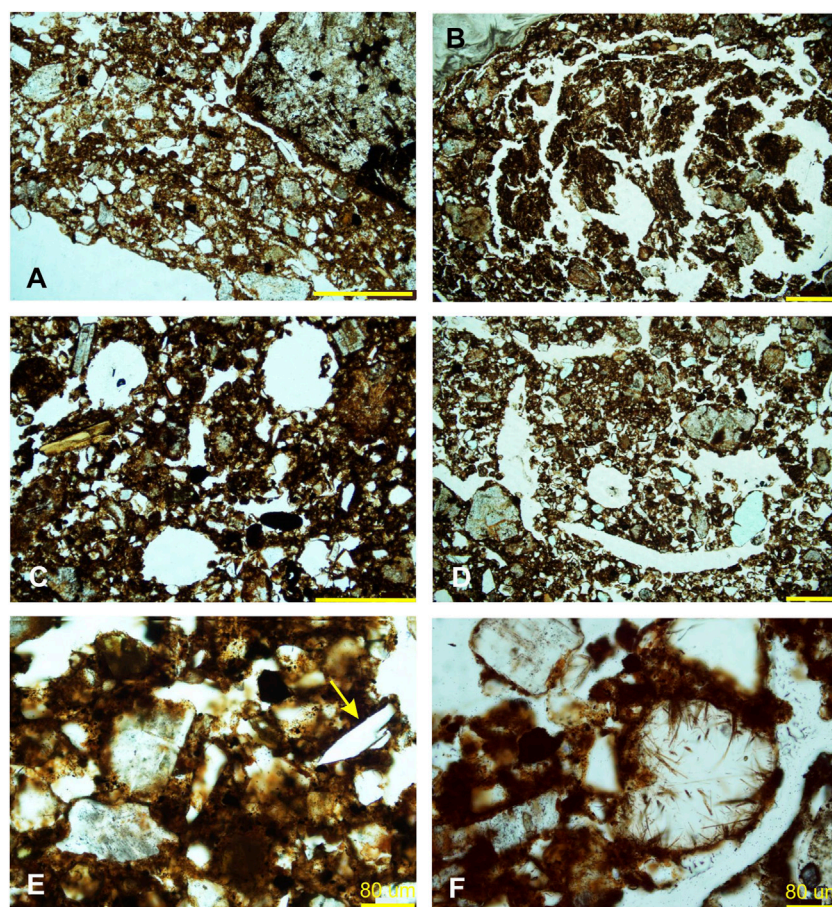


FIGURE 6

Microphotographs of depositional and post-depositional features observed in the Old Geos profile, including (A) rare remnant sedimentary crusts, (B) rotated fabric from faunal activity, (C) open channel voids in amongst dense excremental fabric, (D) collapsed channel feature, (E) quartz shard, and (F) rutilated quartz grain. Yellow scale bar is 600 μm unless otherwise indicated.

Grain size analysis (i.e., based on 2D data) of quartz from TIMA analyses identify a generally constant bimodal profile through this section of Old Geos, with coarse ($\sim 1,000 \mu\text{m}$) and fine sand ($\sim 120 \mu\text{m}$) as the two main modal sizes. The latter is possibly more locally derived and the fine sand more easily transported by runoff. Particle size, as determined using laser analysis on bulk samples, also shows a constant modal distribution throughout the profile, with similar modal peaks at 1,200 μm and 150 μm . There is a greater proportion of the fine sands at 20 cm depth (Figure 5), indicative of infilling of the shell matrix.

3.2 Micromorphology

The micromorphological profile shows the shell-dominated unit grading into the darker red, grain-dominated unit (Figure 3). The upper part of the shell-unit comprises a relatively well-sorted

gefuric fabric, with microcalcites homogeneously mixed with clay aggregates. Sub-rounded quartz grains have fine monic clay coatings, and occasional impregnative Fe- and Mn-oxides in the groundmass. Remnant fine sediment layering or crusts are very rarely preserved (Figure 6A). In the lower part of the profile, the sediments show an increasing excremental fabric with dense microaggregates (Figure 6B), complex packing voids with many channels (Figure 6C) or passage features (Figure 6D) most likely from insect activity. Also present in the sediment matrix, are occasional micro-shards ($< 200 \mu\text{m}$) of quartz (e.g., Figure 6E) that may be cultural in origin; and sub-rounded to rounded grains ($< 120 \mu\text{m}$) of rutilated quartz (quartz which contains needle-like inclusions of rutile, Figure 6F). The latter are not cultural and represent the weathered product from either a hydrothermal or high-grade metamorphic source.

Mirroring the macro-scale record, *Tegillarca* sp. shell (Figure 7A) is clearly dominant in the upper part of the profile, with very occasional evidence of *Terebralia*

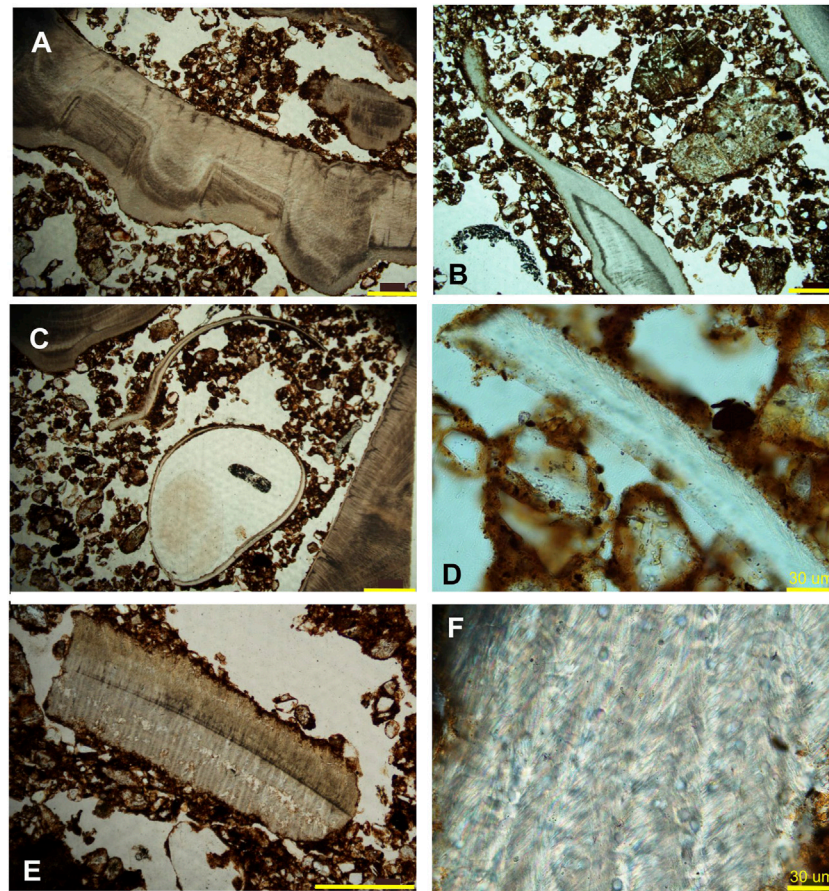


FIGURE 7

Microphotographs of bone fragments in the Old Geos profile, including (A) *Tegillarca* sp. shell, (B) *Terebralia* sp. shell, (C) unidentified shell, (D) unburnt eggshell, (E) decalcified shell fragment, and (F) microbial borings within a shell fragment. Yellow scale bar is 600 μm unless otherwise indicated.

sp. (Figure 7B) and other unidentified shell types (e.g., Figure 7C). Towards the base of the profile where sediments are slightly more acidic, there is evidence of decalcification (Figure 7E) and microbial degradation of shell (Figure 7F). Occasional micro-fragments of eggshell are also present, more towards the base of the sampled profile (Figure 7D) but very few of either the marine or eggshell fragments appear to have been burnt. Conversely there are few (up to 10%) small (<500 μm) fragments of burnt and unburnt bone, increasing in abundance towards the base of the sampled profile. These bones range in colour from pale yellow (Figure 8A), through to the more occasional, dark reddish brown (Figure 8B). The latter darker colours are indicative of heating temperatures of around 400°C, but most bone fragments show medium yellow colour consistent with heating temperatures < 300°C (Stiner et al., 1995; see also Moody et al., 2022).

Some of the bone fragments can be identified as fish bone from the bone structure (e.g., Figure 8C) and serrated edges (e.g.,

Figure 8D). Other fine bones (e.g., Figures 8A,E,F) may be fish or bird bone, whilst porous cancellous bone (e.g., Figure 8G) is consistent with the marine turtle bone which is abundant in the site's faunal assemblage (McDonald et al., 2022). A single sponge spicule (Figure 9D) provides further evidence of transport of non-economic marine resources to this elevated site, probably these were attached to economic species intentionally collected. More massive bone fragments (e.g., Figures 8B,H) may be mammal bone. A few bones (e.g., Figure 8H), also show longitudinal fracturing indicative of weathering and transverse fractures that may be indicative of trampling, whilst towards the base of the profile, bone fragments show clear evidence of microbial degradation and demineralization (.

Plant material includes carbonised (Figures 9A,B) and lesser uncarbonised fragments. Fragments of the former are generally very small (<100 μm) and show little or no cellular structure. Uncarbonised monocotyledon plant fragments also tend to be small (<200 μm) or finely comminuted and cannot be identified;

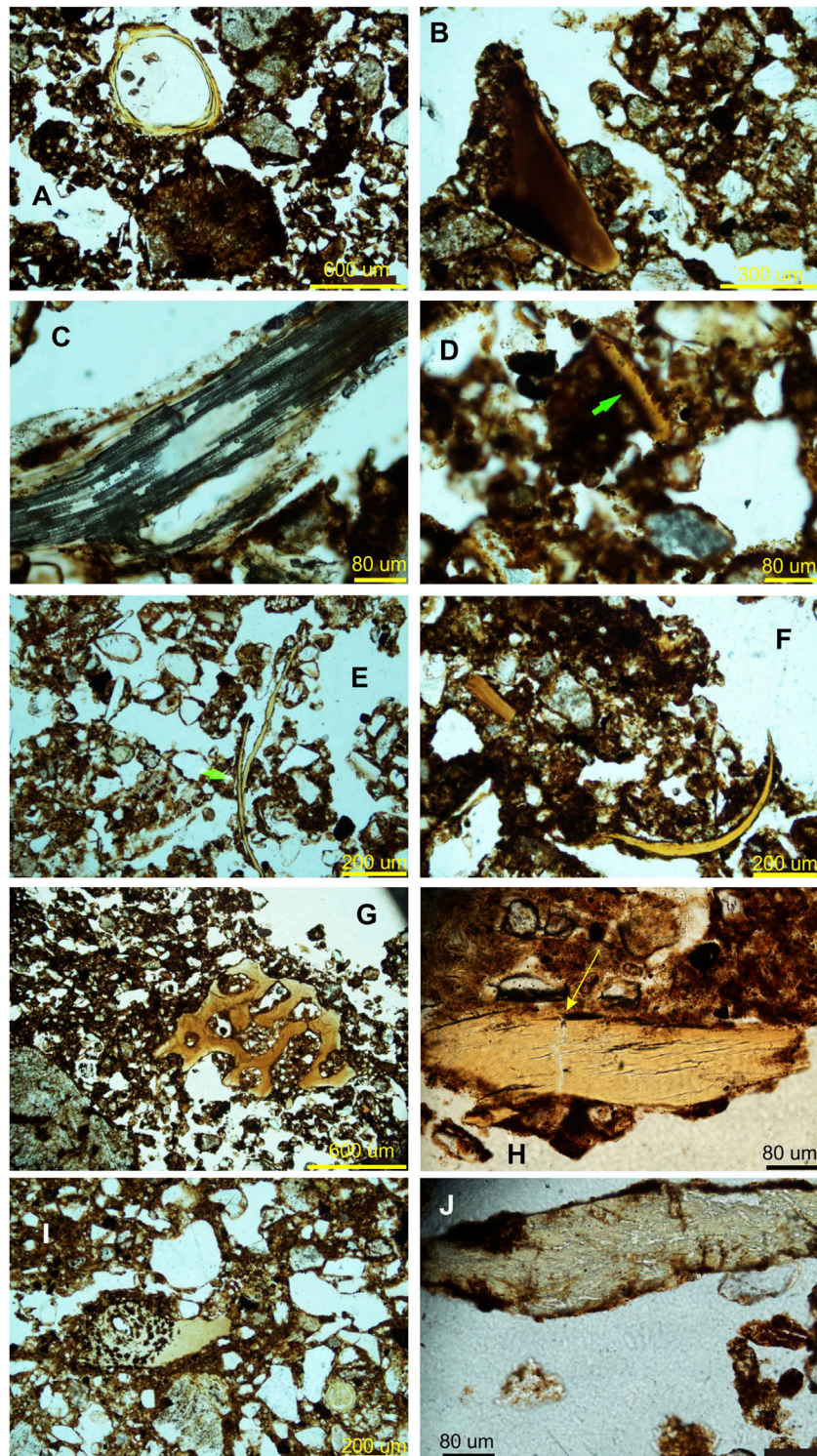


FIGURE 8

Microphotographs of bone remains in the Old Geos profile, including (A) med-yellow, circular (fish?) bone, (B) dark brown burnt bone, (C) degraded fish bone, (D) burnt fish bone with serrated-edge, (E) fine bone, possibly avian, (F) dark yellow, fine bone, (G) dark yellow spongy turtle bone, (H) heated and fractured (mammal) bone, (I) cross-section of bone showing microbial degradation, and (J) bone fragment also showing evidence of microbial degradation.

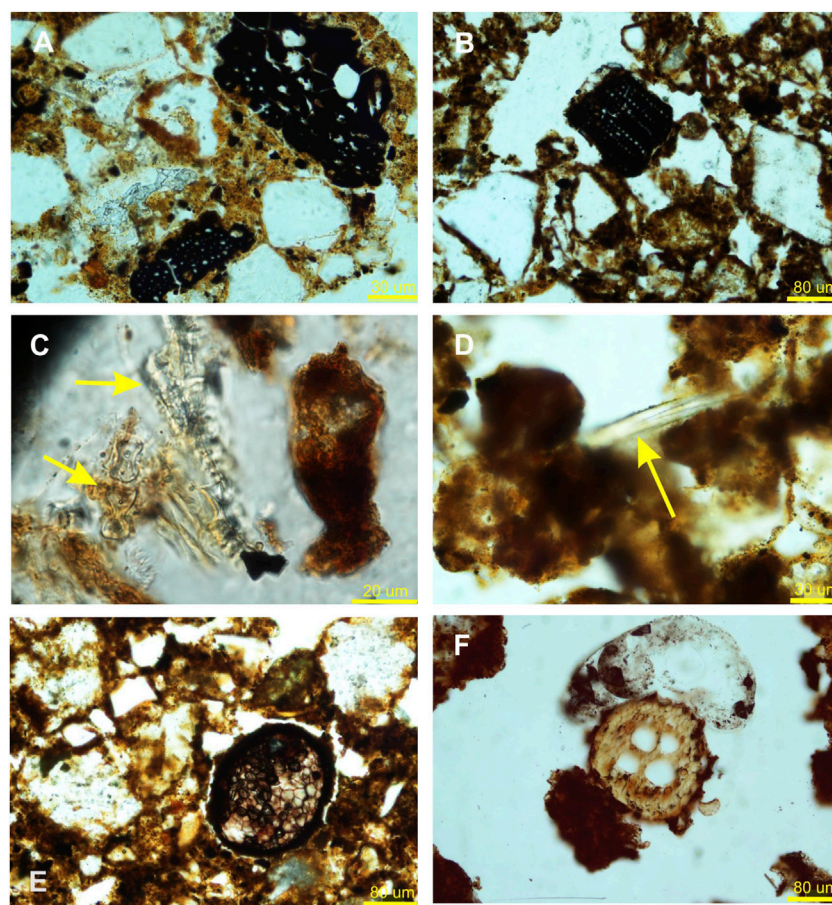


FIGURE 9
Microphotographs of plant remains in the Old Geos profile, including (A) degraded charcoal fragments, (B) vesicular charcoal fragment, (C) dumbbell-shaped wood phytolith, (D) sponge spicule, cut parallel to axial canal, (E) fungal spore, and (F) possible fungal spore.

but there is rare occurrence of plant phytoliths (Figure 9C). In addition, Figure 9E (and possibly also Figure 9F) shows fungal tissue, probably a fruiting body (sclerotium) and is evidence of degrading organic matter.

4 Discussion

4.1 Comparison with macro-scale archaeology

The microanalytical data is generally in accordance with the macro-scale archaeological remains documented in square OG 28690, which identified marine shell, and bone fragments from mammals, marine turtle and fish but also small quantities of echinoderm (sea urchin) spines, and fragments of crustacea (McDonald et al., 2022: Table 15.10, Table 15.12). Mammal bones are predominant (>85%) throughout the macro-bone assemblage (McDonald et al., 2022) and in the observed

micro-analytical record. Micromorphological analysis shows clear evidence of microbial degradation and decalcification of bone, consistent with the slightly more acidic sediments (pH 6.5) at the base of the profile, consistent with observations made during the faunal analysis (McDonald et al., 2022: 20–22).

The macro-bone analysis recorded that 88% of the upper analytical unit was unburnt (McDonald et al., 2021: Table 15.11), with micromorphological observation similarly indicating <10% of bone is burnt. The micro-analysis indicates heating at low temperature (<400°C), with the macro-bone record providing only a few specimens of calcined mammal bone that might indicate higher temperatures in each of the two analytical units (see Stiner et al., 1995; Moody et al., 2022). Natural fires move rather rapidly, and do not bake sediments very deeply (Clements, 2018). Whilst it is possible that at least some of the micro-bone fragments were burnt after they were deposited in the soil, the predominance of macropod species (mainly *Petrogale* sp. or rock wallaby) in the macro-bone assemblage (McDonald et al.,

2022) supports a cultural origin of the bone, with bone colours reflecting burning of still-fleshed bone (Moody et al., 2022).

The shell similarly shows little evidence of being burnt but marine shell only requires low heating temperatures to open. The formation of *Tegillarca* sp. shell midden over older accumulations of *Terebralia* spp. shell is common for this region (Clune and Harrison, 2009), and even the small amounts of *Terebralia* sp. shell in the Old Geos site is indicative of exploitation of coastal mangroves earlier in the Holocene. People were exploiting both marine coastal (fish and turtles) and terrestrial fauna, including possibly birds, that would have been available around this waterhole.

Processing of food is indicated from residue analysis of the stone tool assemblage, over half of which was comprised of locally available rhyodacite (as confirmed from pXRF analysis) (McDonald et al., 2022). Quartz artefacts comprise the next most common material type, while smaller proportions of chalcedony and chert occur throughout the more recent cultural layer. Examples of very small (<200 µm) angular quartz and chalcedonic grains, some with edges indicative of conchoidal fracturing, are consistent with micromorphological features of knapped lithic artefacts (Angelucci 2010, 2017), suggesting the on-site knapping of these materials (Andrefsky 2010).

Charcoal fragments are small (<100 µm) and, whether derived from natural or cultural burning, could have been transported by wind or water (as runoff) from the surrounding area (as may also some of the small bone fragments). Two charcoal samples found in association with shell were found to be so severely altered that insufficient of the original carbon remains for reliable radiocarbon dating (McDonald et al., 2022), as was similarly found for the Nauwalabila site in Northern Territory (Fifield et al., 2001).

Overall, the archaeological data for the Old Geos site complex provides evidence of broad-scale occupation, including artefact manufacture and food consumption. The exact function or functions of the low circular structures is unknown but the similarity in occupation evidence from within the structure compared with that from the open midden site indicates a similarly domestic interpretation. The greater taphonomic disturbance to the sequence inside the circular structure led McDonald et al. (2022) to infer that occupation may have been more intensive within the structure.

4.2 Site formation

TESCAN TIMA, like other automated SEM-based instruments (e.g., MLA-SEM, QEMSCAN) can help to identify mineral phases that provide data on provenance, and also diagenetic phases that provide data on physio-chemical conditions within archaeological sediments.

Mineral analyses from TIMA indicate most of the large rock fragments are alkaline, reflecting the granophyre and granodiorite bedrock geology. The presence of rutilated quartz is an indication of a possible nearby hydrothermal mineral deposit but the rounded nature of these grains (and the majority of other quartz grains) indicates they were most likely transported here by sheet runoff and are not remnants of stone tool manufacture. Dampier Archipelago is subject to annual cyclonic conditions, hence runoff events are episodic and intense rather than regular.

As found elsewhere on the Burrup Peninsula, alkali feldspars (including albite, microcline and orthoclase), and quartz are the main constituents of the sediments (Donaldson 2011; McDonald et al., 2018). TIMA does not distinguish orthoclase and microcline (both $KAlSi_3O_8$) but petrographic analysis indicates orthoclase is the more common phase. The felsic igneous rocks in this region typically very alkaline (Na_2O and K_2O) (Donaldson 2011), and the higher relative abundance of alkali feldspar in the top 10 mm of the profile most likely reflects more freshly weathered material at the ground surface. Regional sediments are also relatively rich in calcite, and travertine deposits are common in the elevated gabbro- and granophyre hillslopes (Donaldson 2011). The homogeneously poorly-sorted, coarse to fine sand likely accumulated between the boulder talus through runoff, with rare remnant crustal layers (Figure 6A) indicating accumulation was episodic rather than continuous. The boulders, cobble and shell provide a relatively stable clast-supported framework, limiting the movement of pebble size or larger material. Sediments accumulate within and around this framework and over time undergo diagenesis (including ferruginisation) and localised reworking by ants or termites.

Diagenetic phases include micro-calcites (fine calcite) and clays (aluminosilicates), with the latter characterised by the incorporation of Mg, K, Ca, Na, Fe, Zn, V ions into their structures. Intense insect activity is evident from excretory fabric, channel voids, and finely comminuted organics and limits soil development and formation of clay and carbonate pedofeatures (e.g., concretions, coatings). Field observation suggests such activity may be continuous throughout the profile with soil moisture a limiting factor to subterranean termites, which have little resistance to dehydration. Micromorphological analysis indicates degradation of bone and shell is both chemical (through decalcification) and biological, with sufficient soil moisture and acidity buffered enough (perhaps by carbonates and clay) to allow fungal activity to have occurred sometime in the past. Whilst post-depositional and syn-depositional disturbance of archaeological sites by invertebrates is likely to be the norm (Williams, 2019), the indication from this study is that disturbance is mainly concentrated between the shell matrix and the entire archaeostratigraphy has not been lost.

4.3 Usefulness of micro-analytical, including automated mineral, studies of archaeological sites in this region

Macroscopic analysis of the midden deposit, including identification and quantification of cultural material, has provided a broad understanding of the nature and resolution of the Old Geos site in the late Holocene. Microscopic methods, including use of automated mineral analysis and micromorphology, are capable of isolating depositional events at exceptionally fine resolution (e.g., Villagran et al., 2011a, 2011b; Godino et al., 2011; Brown et al., 2021) but only when this resolution is preserved. In the case of the Old Geos site, fine resolution is limited by the process of infilling of the boulder talus and further complicated by post-depositional reworking, with only rare remnants preserved. Micro-analytical techniques can provide some assessment of the degree of disturbance and age-mixing in the deposits but, as Parker et al. (2020) demonstrate, higher-resolution dating would provide a more robust empirical assessment. Whilst the statistically equivalent ages within the *Tegillarca* sp.-rich shell unit provides some confidence in the temporal resolution of the upper analytical unit, despite evident bioturbation, the extent of time-averaging (on a multimillennial scale) of the second analytical unit is less clear. Micro-analytical investigation of this lower unit would help resolve the extent of this and it has only been possible to consider broad processes within the aggregated deposit (see also Parker et al., 2020; Koppel et al., 2021).

Automated mineral analysis is also useful for differentiating some inorganic components within the midden site, in particular igneous minerals that largely indicate localized weathering. Less success, however, was had with differentiating compositionally similar minerals and in particular shell type, as well as burnt and unburnt, or post-depositionally altered cultural phases. For shell type, whole shell analysis using XRD or XRF (or on site pXRF) may provide a better mineral or geochemical reference, and this may be explored in future studies. For shell heating, the combined use of micromorphology, XRD and FTIR (Fourier Transform Infrared) could be useful (Aldeias et al., 2016).

The accurate, automated, and quantitative analyses of minerals provided by SEM-based mineral identification techniques removes inherent biases from human observation. This is very apparent in the abundance of bone (apatite) as determined visually from micromorphology (<10%), which is significantly greater than that estimated empirically by TIMA (<1%). The former may partly be attributed to observer bias of bone within particular magnifications of the thin sections using visual estimate charts, with a 5–10% range between groupings (e.g., Rothwell 1989; Stoops 2003; Stevenson 2012). As Stoops (2003: 49) notes, the same percentage abundances can be more or less significant for different mineral phases in different

depositional contexts. The minor inosilicates (e.g., actinolite/ferro-actinolite), mica (biotite, muscovite) and heavy mineral (e.g., rutile, zircon) phases reflects the source mineralogy and indicate that weathering has not significantly affected the mineral assemblage that may be taken into the transport system. In contrast, on nearby Barrow Island, the abundance of (minor) heavy mineral phases is a significant indicator of weathering and sediment maturity (Ward et al., 2022).

Our use of automated mineralogical analysis for the Old Geos site is constrained by the single dataset, which although likely to be analytically accurate (Pirrie et al., 2009) provides limited assessment of variability within the sequence or with the sediment profile within the low stacked circular structures. Questions also remain as to how this midden site differs from those found in closer proximity to marine, estuarine and less often, freshwater bodies, in this region. Comparison with the TIMA (Ward et al., 2018) and micromorphological analysis (Ward et al., 2017) of sediments from the site of Boodie Cave on Barrow Island, 120 km to the west (Figure 1) demonstrates the advantage of a larger dataset to explore continuity and change in archaeological deposits, particularly in relation to sea level change. However, both sites do at least show fairly steady sediment source and transport processes over the last 7,000 years, when sea levels stabilized around modern levels.

5 Conclusion

This study forms a pilot for micro-analytical investigation of middens, shell and earth mounds within the arid coastal Pilbara region and elsewhere, including use of automated mineral analysis and micromorphology. Automated mineral analysis allows for coarse chemical differentiation of the igneous rocks and sedimentary matrix and is significantly aided by micromorphological investigation to help differentiate compositionally similar minerals, shell species, and differentially altered cultural phases within the profile. Although the sedimentary matrix has been significantly reworked by invertebrates, the combined macro- and micro-analytical data still provides a coherent record of archaeological site formation and cultural activity at this elevated site over the late Holocene. More significant change may be revealed from deposits and midden sites that relate to before sea level stabilization. It is hoped that this pilot might prompt further studies to help fill the current research gap in terms of high-resolution micro-analytical studies of shell midden sites in Australia.

Data availability statement

The raw data supporting the conclusions of this article will be made available by the authors, without undue reservation.

Author contributions

IW was responsible for conceptualisation, micromorphological field sampling, methodology and formal analysis—TIMA and micromorphology, funding of TIMA analyses, writing the original draft and production of figures; JM was responsible for funding acquisition, project conceptualisation, direction of field excavation and lab macro-analysis, review and editing of the manuscript; JF assisted with mineralogical analysis, and undertook review and editing of the manuscript; CM did the analysis of the macro-faunal remains and assisted in identification of some of the micro-fragments of bone, and also undertook review and editing of the manuscript.

Funding

Fieldwork was funded by Australian Research Council (ARC) Linkage Project LP140100393 Administered by UWA with partner organisation Rio Tinto Iron Ore (RTIO) and collaborating organization Murujuga Aboriginal Corporation. Ingrid Ward is supported by Australian Research Council Discovery Early Career Researcher Award Fellowship (DE180100601). The Tescan TIMA FEG-SEM with four PulsTor SDD X-ray detectors at the John de Laeter Centre was acquired through Australian Research Council LIEF grant LE140100150.

References

- Aldeias, V., Gur-Arieh, S., Maria, R., Monteiro, P., and Cura, P. (2016). Shell we cook it? An experimental approach to the microarchaeological record of shellfish roasting. *Archaeol. Anthropol. Sci.* 11 (2), 389–407. doi:10.1007/s12520-016-0413-1
- Andrefsky, W. (2010). Human land-use strategies and projectile point damage, resharpening, and discard patterns. *Hum. Evol.* 25 (1-2), 13–30.
- Angelucci, D. E. (2017). "Lithic artefacts," in *Archaeological soil and sediment micromorphology*. Editors C. Nicosia and G. Stoops (New Jersey: Wiley Blackwell), 223–230.
- Angelucci, D. E. (2010). The recognition and description of knapped lithic artifacts in thin section. *Geoarchaeology* 25, 220–232. doi:10.1002/gea.20303
- Beckett, E. (2021). *Contextualising Murujuga stone structures: Dampier archipelago*. Unpublished PhD thesis, Crawley: Centre for Rock Art Research + Management, and Archaeology, University of Western Australia.
- Brown, A. G., Van Hardenbroek, M., Fonville, T., Davies, K., Mackay, H., Murray, E., et al. (2021). Ancient DNA, lipid biomarkers and palaeoecological evidence reveals construction and life on early medieval lake settlements. *Sci. Rep.* 11, 11807. doi:10.1038/s41598-021-91057-x
- Clements, C. B. (2018). Thermodynamic structure of a grass fire plume. *Int. J. Wildland Fire* 19 (7), 895–902. doi:10.1071/wf09009
- Clune, G., and Harrison, R. (2009). Coastal shell middens of the Abydos coastal plain, Western Australia. *Archaeol. Ocean.* 44, 70–80. doi:10.1002/j.1834-4453.2009.tb00069.x
- Donaldson, M. (2011). Understanding the rocks: Rock art and the geology of Murujuga (Burrup 'Peninsula'). *Rock Art Res.* 28 (1), 35–43.
- Fifield, K., Bird, M. I., Turney, C. S. M., Hausladen, P. A., Santos, G. M., and di Tada, M. L. (2001). Radiocarbon dating of the human occupation of Australia prior

Acknowledgments

We are grateful for the support of the Circle of Elders advising the Murujuga Aboriginal Corporation (MAC). We also thank Peter Veth, Audrey Vincent, Victoria Anderson, Sarah de Koning, Joe Dortch, Al Paterson and Peter Ross who participated in the excavations of the Old Geos site. Joe Dortch drew the original sections and supervised the lab volunteers who sorted the shells; Kelly Merigot ran the TIMA analyses at John de Laeter centre and both she and Tommaso Tacchetto assisted in the analysis of the results. Finally we thank the three anonymous reviewers for their helpful comments.

Conflict of interest

The authors declare that the research was conducted in the absence of any commercial or financial relationships that could be construed as a potential conflict of interest.

Publisher's note

All claims expressed in this article are solely those of the authors and do not necessarily represent those of their affiliated organizations, or those of the publisher, the editors and the reviewers. Any product that may be evaluated in this article, or claim that may be made by its manufacturer, is not guaranteed or endorsed by the publisher.

to 40 ka BP—Successes and pitfalls. *Radiocarbon* 43, 1139–1145. doi:10.1017/s0033822200041795

Godino, I. B., Álvarez, M., Balbo, A., Zurro, D., Madella, M., Villagrán, X., et al. (2011). Towards high-resolution shell midden archaeology: Experimental and ethnoarchaeology in tierra del fuego (Argentina). *Quat. Int.* 239 (1), 125–134. doi:10.1016/j.quaint.2011.04.017

Hrstka, T., Gottlieb, P., Skála, R., Breiter, K., and Motl, D. (2018). Automated mineralogy and petrology – applications of TESCAN integrated mineral analyzer (TIMA). *J. Geosci.* 63, 47–63. doi:10.3190/jgeosci.250

Koppel, B. D., Szabo, K., Moore, M. W., and Morwood, M. (2021). Untangling time-averaging in shell middens: Defining temporal units using amino acid racemisation. *J. Archaeol. Sci. Rep.* 7, 741–750. doi:10.1016/j.jasrep.2015.08.040

McDonald, J. J., and Veth, P. (2009). Dampier archipelago petroglyphs: Archaeology, scientific values and national heritage listing. *Archaeol. Ocean.* 44, 49–69. doi:10.1002/j.1834-4453.2009.tb00068.x

McDonald, J., Reynen, W., Ditchfield, K., Blunt, Z., Monks, C., Beckett, E., et al. (2022). "Excavations on the Burrup: Old Geos and watering cove. Chapter 15," in *Murujuga: Dynamics of the dreaming. Rock art, stone features and excavations across the dampier archipelago. CRAR+M monograph No. 2. Perth: UWAPress*. Editors J. McDonald, K. Mulvaney, A. Paterson, and P. Veth.

McDonald, J., Reynen, W., Ditchfield, K., Dortch, J., Leopold, M., Stephenson, B., et al. (2018). Murujuga rockshelter: First evidence for pleistocene occupation on the Burrup Peninsula. *Quat. Sci. Rev.* 193, 266–287. doi:10.1016/j.quascirev.2018.06.002

Moody, K., Ristovski, N., Manne, T., Ward, I., and Veth, P. (2022). A burning question: What experimental heating of Australian fauna can tell us about cooking

- practices in Boodie Cave, Barrow Island, northwest Australia. *J. Archaeol. Sci. Rep.* 44, 103535. doi:10.1016/j.jasrep.2022.103535
- Morse, K. (2009). Introduction: Emerging from the abyss—archaeology in the Pilbara region of western Australia. *Archaeol. Ocean.* 44, 1–5. doi:10.1002/j.1834-4453.2009.tb00062.x
- Parker, W. G., Yanes, Y., Hernandez, E. M., Hernandez Marrero, J. C., Pais, J., and Surge, D. (2020). Scale of time-averaging in archaeological shell middens from the Canary Islands. *Holocene* 30 (2), 258–271. doi:10.1177/0959683619883020
- Piccoli, P. M., and Candela, P. A. (2002). Apatite in igneous systems. *Rev. Mineralogy Geochem.* 48, 255–292. doi:10.2138/rmg.2002.48.6
- Pirrie, D., Power, M. R., Rollinson, G. K., Wiltshire, P. E. J., Newberry, J., and Campbell, H. E. (2009). “Automated SEM-EDS (QEMSCAN®) mineral analysis in forensic soil investigations: Testing instrumental reproducibility,” in *Criminal and environmental soil forensics*. Editors K Ritz (Springer Science), 411–430. Chapter 26.
- Rothwell, R. G. (1989). *Minerals and mineraloids in marine sediments: An optical identification guide*, Elsevier Applied Science, London, 279. (ISBN 1-85166-382-7).
- Stevenson, J. A. (2012). A visual estimate of the proportions of mixtures: Pumice vs. lithics. Volcano01010. Available at <https://all-geo.org/volcan01010/2012/09/pumicelithicsproportions/>.
- Stiner, M. C., Kuhn, S. L., Weiner, S., and Bar-Yosef, O. (1995). Differential burning, recrystallization, and fragmentation of archaeological bone. *J. Archaeol. Sci.* 22, 223–237. doi:10.1006/jasc.1995.0024
- Stoops, G. (2003). *Guidelines for analysis and description of soil and regolith thin sections*. Wisconsin: Soil Science Society of America, 184.
- Villagran, X. S., Balbo, A. L., Madella, M., Vila, A., and Estevez, J. (2011a). Experimental micromorphology in Tierra del Fuego (Argentina): Building a reference collection for the study of shell middens in cold climates. *J. Archaeol. Sci.* 38 (3), 588–604. doi:10.1016/j.jas.2010.10.013
- Villagran, X. S., Balbo, A. L., Madella, M., Vila, A., and Estevez, J. (2011b). Stratigraphic and spatial variability in shell middens: Microfacies identification at the ethnohistoric site tunel VII (tierra del fuego, Argentina). *Archaeol. Anthropol. Sci.* 3 (4), 357–378. doi:10.1007/s12520-011-0074-z
- Wan Mohammad, W. A. S. B., Nor Hazurina, O., Mohd Haziman, W. I., Masazurah A. R., Shahiron, S., and Raha Abd, R. (2017). A review on seashells ash as partial cement replacement. IOP conference series. *Mater. Sci. Eng.* 271 (1), 12059.
- Ward, I., Larcombe, P., Mulvaney, K., and Fandry, C. (2013). The potential for discovery of new submerged archaeological sites near the Dampier Archipelago, Western Australia. *Quat. Int.* 308–309, 216–229. doi:10.1016/j.quaint.2013.03.032
- Ward, I., Veth, P., Prossor, L., Denham, T., Ditchfield, K., Manne, T., et al. (2017). 50,000 years of archaeological site stratigraphy and micromorphology in Boodie Cave, Barrow Island, western Australia. *J. Archaeol. Sci. Rep.* 15, 344–369. doi:10.1016/j.jasrep.2017.08.012
- Ward, I., Merigot, K., and McInnes, B. I. A. (2018). Application of quantitative mineralogical analysis in archaeological micromorphology: A case study from Barrow is., western Australia. *J. Archaeol. Method Theory* 25 (1), 45–68. doi:10.1007/s10816-017-9330-6
- Ward, I., Vannieuwenhuysse, D., Ditchfield, K., and Barteaux, J. (2019). Western wonders under the microscope: Building a micromorphology reference collection for northwest Australia. *J. R. Soc. West. Aust.* 102, 10–27.
- Ward, I. A. K., Bateman, M. D., Larcombe, P., Scott, P. M., Li, T., Murai, K., et al. (2022). A pilot study into the geochronological and geomorphic context for the archaeology of Barrow Island, Western Australia. *Quat. Int.* doi:10.1016/j.quaint.2022.02.002
- Williams, M. A. J. (2019). Termites and stone lines – traps for the unwary archaeologist. *Quat. Sci. Rev.* 226, 106028. doi:10.1016/j.quascirev.2019.106028